Accessing a growth window for $SrVO_3$ thin films

Matthew Brahlek, Lei Zhang, Craig Eaton, Hai-Tian Zhang, and Roman Engel-Herbert

Citation: Appl. Phys. Lett. **107**, 143108 (2015); doi: 10.1063/1.4932198
View online: https://doi.org/10.1063/1.4932198
View Table of Contents: http://aip.scitation.org/toc/apl/107/14
Published by the American Institute of Physics

Articles you may be interested in

Growth of $SrVO_3$ thin films by hybrid molecular beam epitaxy
Journal of Vacuum Science & Technology A: Vacuum, Surfaces, and Films **33**, 061504 (2015); 10.1116/1.4927439

Self-regulated growth of $LaVO_3$ thin films by hybrid molecular beam epitaxy
Applied Physics Letters **106**, 233102 (2015); 10.1063/1.4922213

Mapping growth windows in quaternary perovskite oxide systems by hybrid molecular beam epitaxy
Applied Physics Letters **109**, 101903 (2016); 10.1063/1.4962388

Metal-insulator transition induced in $CaVO_3$ thin films
Journal of Applied Physics **113**, 133704 (2013); 10.1063/1.4798963

Molecular beam epitaxy of $SrTiO_3$ with a growth window
Applied Physics Letters **95**, 032906 (2009); 10.1063/1.3184767

Growth of high-quality $SrTiO_3$ films using a hybrid molecular beam epitaxy approach
Journal of Vacuum Science & Technology A: Vacuum, Surfaces, and Films **27**, 461 (2009); 10.1116/1.3106610

Accessing a growth window for $SrVO_3$ thin films

Matthew Brahlek, Lei Zhang, Craig Eaton, Hai-Tian Zhang, and Roman Engel-Herbert[a)]
Department of Materials Science and Engineering, Pennsylvania State University, University Park, Pennsylvania 16801, USA

(Received 14 July 2015; accepted 22 September 2015; published online 6 October 2015)

Stoichiometric $SrVO_3$ thin films were grown over a range of cation fluxes on (001) $(La_{0.3}Sr_{0.7})(Al_{0.65}Ta_{0.35})O_3$ substrates using hybrid molecular beam epitaxy, where a thermal effusion cell was employed to generate a Sr flux and V was supplied using the metal-organic precursor vanadium oxytriisopropoxide (VTIP). By systematically varying the VTIP flux while keeping the Sr flux constant, a range of flux ratios were discovered in which the structural and electronic properties of the $SrVO_3$ films remained unaltered. The intrinsic film lattice parameter and residual resistivity were found to be the smallest inside the growth window, indicating the lowest defect concentration of the films, and rapidly increased for cation flux ratios deviating from ideal growth condition. Reflection high-energy electron diffraction showed that films grown within this range had smooth surfaces and diffraction patterns were free of additional spots, while otherwise the growing surface was rough and contained additional crystalline phases. Results show the existence of a $SrVO_3$ growth window at sufficiently high growth temperature, in which high-quality, stoichiometric films can be grown in a robust, highly reproducible manner that is invulnerable to unintentional flux variation. © *2015 AIP Publishing LLC*.
[http://dx.doi.org/10.1063/1.4932198]

Transition metal oxides (TMOs) abound with a variety of novel electronic phases due to the many competing energy scales,[1] which can stabilize high-temperature superconductivity close to magnetic phases,[2] and insulating states in close proximity to metallic states.[3] The ability to switch between disparate electronic ground states can enable new functionalities in electronic devices that are relevant in practical applications.[4,5] It has therefore remained in the focus of fundamental research to gain a better understanding of the underlying principles. However, progress towards employing TMOs in applications and understanding electronic phase transitions is hampered by the difficulties in controlling stoichiometry during growth and the resulting lack of overall reproducibility of film properties. For example, stoichiometric $SrVO_3$ has been shown to be a highly conductive metal,[6] exhibiting strong electron correlation effects[7] that can be epitaxially integrated with other oxides.[8] $SrVO_3$ films have previously been grown by pulsed laser deposition,[9–11] pulsed electron evaporation,[12] chemical vapor deposition,[9] and more recently by hybrid molecular beam epitaxy (hMBE).[6,13] However, unintentional disorder introduced during growth in the form of defects dramatically deteriorate film properties,[14,15] e.g., substantially increase the resistivity. Therefore, it is necessary to identify better suited synthesis methods and optimal growth conditions to obtain high quality $SrVO_3$.

One promising approach towards this goal to grow thin film TMOs is to adapt the well-established strategy for the growth of compound semiconductors. In particular, MBE has enabled the growth of films with unprecedented quality, such as GaAs.[16] The key to achieving such levels of material perfection is that GaAs coexists with its vapor phase for a wide range of temperatures under As-rich conditions due to the high vapor pressure of As, and that the targeted phase is a line-compound[17]—the Gibbs free energies for the formation of parasitic, non-stoichiometric defect phases is larger than the pure phase. This favorable growth mechanism, enabled by the volatility of As, allows excess As to desorb off the growing surface rather than being incorporated into the crystal lattice as defects; this adsorption-controlled effect is referred to as a growth window because the defect-free structure can be formed over a range of Ga-to-As ratios. Electron mobilities in GaAs based materials in excess of $\sim 36\,000\,000\,cm^2/V\,s$ are a true testament of the success employing this approach, achieving a level of material perfection that is unparalleled by any other synthesis technique.[18]

In contrast, ternary TMOs, such as ABO_3 perovskites like $SrVO_3$, have proven far more difficult to be grown by MBE. A growth window can only be found for a few limiting cases, where the film is made from constituents with high volatilities, e.g., Pb- and Bi-based perovskite compounds such as $BiFeO_3$,[19] $PbTiO_3$,[20] and $BiMnO_3$.[21] In the absence of a volatile component, which could enable film growth in a self-regulated fashion,[22] the A-to-B cation stoichiometry is achieved manually through careful calibration of the individual fluxes, typically limiting the film cation stoichiometry to ~1% accuracy. The manual calibration can be particularly challenging because growth often requires high oxygen partial pressures, causing cation flux drifts during the growth due to surface oxidation of the metal charge inside the effusion cell, as in the case of alkaline earth elements.[23]

The hMBE technique has been found to simplify the growth of TMO perovskites.[24,25] In contrast to conventional

[a)]Author to whom correspondence should be addressed. Electronic mail: rue2@psu.edu

 © 2015 AIP Publishing LLC

MBE, where all cations are supplied by thermal evaporation in either molecular oxygen, atomic oxygen, or ozone, hMBE differs in that only *one* of the elements, typically the A-site cation, is supplied by thermal evaporation using an effusion cell, while the second cation is supplied in the form of a metal-organic molecule[24,26]—analogous to chemical beam epitaxy and metal-organic MBE.[27,28] The volatility of the metal-organic precursor can enable the desired self-regulated growth window, which allows the growth of stoichiometric films over a range of cation fluxes.[22] The quality of the TMO films grown by hMBE have yielded record high carrier mobility, and thus low defect density, in $SrTiO_3$,[29] record high residual resistivity ratio (RRR) in metallic $SrVO_3$,[6] and the lowest cross-over temperature of the weakly localized 2D electron gas at $NdTiO_3/SrTiO_3$ interfaces.[30]

Although previous studies on the growth of $SrVO_3$ by hMBE at a lower substrate temperature of 800 °C did not reveal the existence of a growth window,[6] the discovery of a self-regulated growth window for $LaVO_3$ thin films[31] has motivated the search for a $SrVO_3$ growth window. Here, we report that by increasing the growth temperature to 900 °C, a growth window for $SrVO_3$ can be accessed, which allows the growth of stoichiometric $SrVO_3$ over a range of Sr to vanadium oxytriisopropoxide (VTIP) flux ratios (Sr/VTIP). Lattice parameter expansion and electronic transport properties using low temperature resistivity were used as a direct probe of the defect concentration in the films, revealing similar trends. A well-defined minimum of lattice parameter and residual resistivity across the entire range of flux ratio was found, which sharply increased outside these bounds, constituting the growth window. This shows that high-quality stoichiometric $SrVO_3$ thin films can be grown in a robust, highly reproducible manner, which is insensitive to small errors inherent to flux calibration measurements.

50 nm thick $SrVO_3$ films were grown[32] using a DCA M600 hMBE system, which, as shown schematically in Fig. 1, is equipped with a thermal effusion cell to supply Sr, and gas inlet systems used to supply oxygen and VTIP separately. The gas inlet system used to supply V consisted of a reservoir of liquid VTIP, which was connected to the gas injector nozzle by a variable leak valve.[25] To prevent clogging of the lines, the gaseous VTIP molecules were kept from condensing on the inner walls by heating the entire setup to an elevated temperature ($T_{VTIP} = 70$ °C). To control the amount of VTIP injected into the growth reactor, the pressure of the VTIP supply line (P_{VTIP}) was kept constant by adjusting the variable leak valve in real-time using an automated feedback loop between the leak valve and a capacitance manometer. Herein, we will refer to the samples by the only growth parameter varied, the foreline pressure, P_{VTIP}, in mTorr, which was systematically varied between 40.0 and 65.0 mTorr. It is noted that inside the hMBE reactor, the background pressure of VTIP inside the MBE remained less than $\sim 10^{-8}$ Torr.

The lattice parameter has been found to be a good indicator of the defect concentration in perovskite oxides related to cation stoichometry[31,33,34] and can therefore be used to identify a growth window. We show in Fig. 2 results from high-resolution X-ray diffraction (XRD) 2θ-ω scans around the 002 peak of $(La_{0.3}Sr_{0.7})(Al_{0.65}Ta_{0.35})O_3$ (LSAT) and $SrVO_3$ performed with a Phillips X'Pert Panalytical Pro

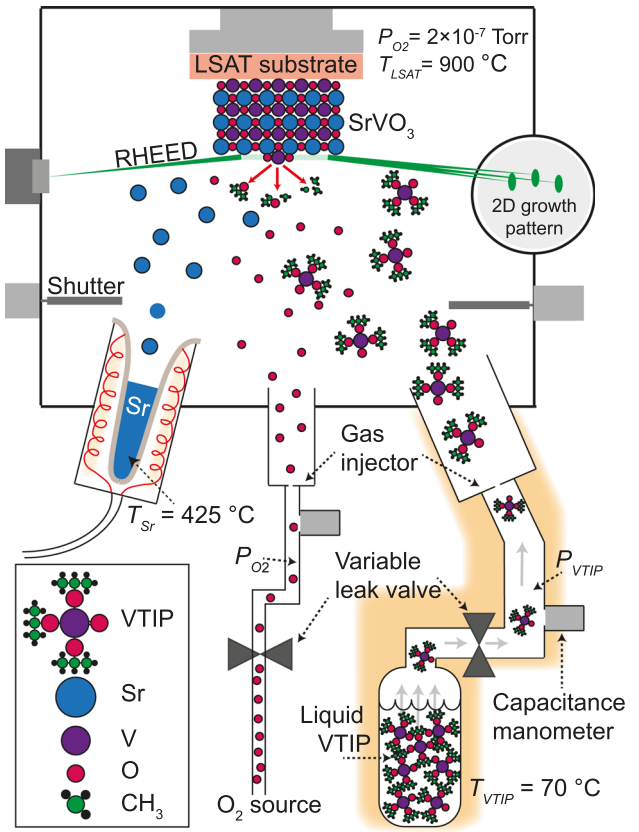

FIG. 1. Schematic of the hybrid molecular beam epitaxy (hMBE) setup used to grow stoichiometric $SrVO_3$. Moving from left to right: strontium (Sr, represented by large blue circles) was supplied by a thermal cell, molecular oxygen (O, small red circles) was supplied using a gas injection system that is maintained at a constant pressure P_{O2}, and vanadium was supplied by the metal-organic vanadium oxytriisopropoxide (VTIP, $VO(OCH(CH_3)_2)_3$) using a gas injection system that is maintained at a constant temperature, $T_{VTIP} = 70$ °C, and pressure, P_{VTIP}. P_{O2} and P_{VTIP} were monitored by a capacitance manometer and held constant by adjusting a variable leak valve in real time.

using Cu-$K_{\alpha 1}$ radiation. Thickness and intrinsic lattice parameter were extracted from the 2θ-ω data from the periodicity of the Kiessig fringes and the $SrVO_3$ 002 peak position.[33] Plotted in Fig. 2(b) is the intrinsic lattice parameter, $a_F = 2\nu/(1+\nu)a_{sub} + (1-\nu)/(1+\nu)a_c$, where a_c is the film's out-of-plane lattice parameter extracted from the 002 peak position, $a_{sub} = 3.868$ Å is the in-plane lattice parameter of LSAT, and $\nu \approx 0.28$ is the Poisson ratio of $SrVO_3$.[6] Between 45.0 and 52.0 mTorr, the lattice parameter of $SrVO_3$ was found to be the smallest and constant, indicating a minimum point defect concentration that was independent of P_{VTIP}. We define this region of P_{VTIP} to be inside the growth window. Outside the growth window, the intrinsic lattice parameter of $SrVO_3$ increased with increasing deviation of P_{VTIP} from the growth window. $SrVO_3$ grown with excess VTIP have been found to be V-rich with rocksalt VO_x intergrowths as the predominant defect while for VTIP deficient condition, excess Sr was accommodated into the lattice by the formation of Ruddlesden-Popper type defects.[13] Further, as shown in Fig. 2(a), Kiessig fringes were present over a wide range of P_{VTIP}, indicating that the film surface and interfaces were flat. Thickness fringes were also observed for films outside the growth window, and disappeared for $P_{VTIP} < 45.0$ mTorr, and $P_{VTIP} > 55.0$ mTorr. From the Kiessig fringes of films

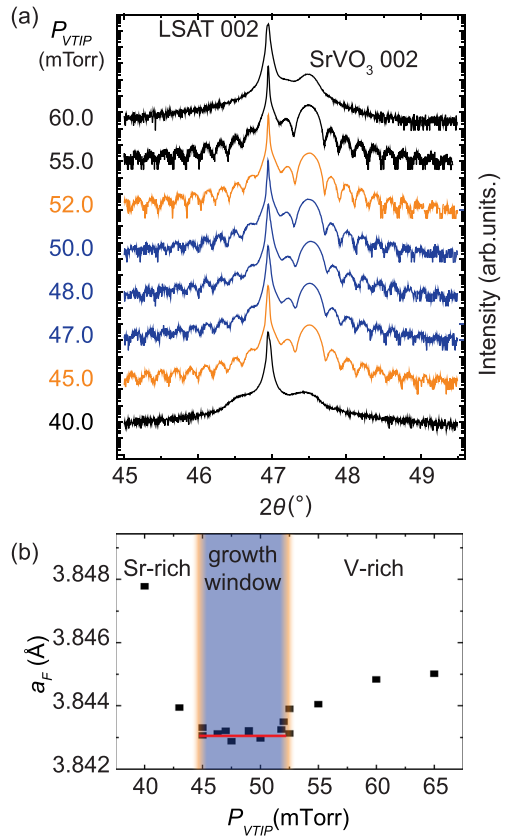

FIG. 2. (a) X-ray diffraction 2θ-ω scans taken around the 002 peaks of $SrVO_3$ and LSAT (the 2θ-ω curves have been offset vertically for clarity), and (b) the intrinsic lattice parameter of $SrVO_3$ extracted from the XRD film peak position. The blue shaded area highlights the growth window, while the orange lines indicate the growth window edges.

grown inside the growth window the film thickness was extracted and was found to be constant at a value of 49 ± 1 nm over a range of P_{VTIP} from 45.0 to 55.0 mTorr. The ~1 nm uncertainty (2% relative error) in the film thickness was attributed to the ~2% error of the Sr flux calibration that is inherent to the quartz crystal microbalance (QCM) measurements (see next).

At the edges of the growth window different values of the intrinsic lattice parameter were obtained for different growths using the same P_{VTIP}. These fluctuations of the film lattice parameter were attributed to the uncertainty of the P_{VTIP}/Sr flux ratio. The deviation in P_{VTIP} during growth was less than ± 0.1 mTorr, whereas the estimated error of Sr flux calibration using the QCM was around $\pm 2\%$, determined from the thickness variation inside the growth window, i.e., $(2.50 \pm 0.05) \times 10^{13}\,\mathrm{cm}^{-2}\,\mathrm{s}^{-1}$. It was the largest source of error in the P_{VTIP}/Sr flux ratio, giving rise to the different values at the edges. For example, on the V-rich edge of the growth window ($P_{VTIP} \approx 52.5$ mTorr) an unintentionally higher Sr flux gave rise to stoichiometric growth conditions with a film lattice parameter of 3.843 Å, and an unintentionally lower Sr flux gave rise to a film with $a_F = 3.844$ Å. The ~2% error of Sr flux calibration can be converted into a finite growth window edge of ~1 mTorr. From these XRD results, it is concluded that inside the growth window of $P_{VTIP} \approx 45.0$–52.0 mTorr, films were stoichiometric constituting a growth window 7 times larger than the uncertainty inherent to QCM measurements.

To further corroborate the determination of stoichiometric films relying on structural characterization, temperature dependent electrical resistivity measurements were employed. Low temperature resistivity, which is dominated by electron scattering from lattice imperfections, is a sensitive probe to quantify the defect concentration in the films. Four-point probe measurements in the van der Pauw geometry were performed on all films from 300 K down to 5 K using pressed indium wires as contacts. Figure 3(a) shows the temperature dependent resistivity for the series of films. The resistivity curves for films within the growth window, as defined by XRD, were similar, whereas films grown outside the window were dependent on P_{VTIP}. The residual resistivity ratio $RRR = \rho(300\,\mathrm{K})/\rho(5\,\mathrm{K})$ was used to quantify the degree of disorder and defect concentration in $SrVO_3$ and is shown in the inset. A plateau within the growth window $P_{VTIP} \approx 45.0$–52.0 mTorr was found, which exhibits the highest *RRR*, and, thus, the smallest contribution of defect scattering to transport. The degree of disorder was the lowest and independent of the Sr/VTIP flux ratio, directly indicating the existence of a self-regulated growth mechanism. It is further noted that the consistency of *RRR* inside the growth window was much better compared to the edges of the growth window. On direct comparison of *RRR* to films grown previously at lower temperature,[6] values reported here were lower by about a factor of 2; 125 versus 222. This smaller *RRR* can be attributed to the higher growth temperature, which may cause addition oxygen vacancies; increasing the oxygen partial pressure during growth, or post-growth annealing will likely help, but will require a further study.

Figure 3(b) shows the resistivity plotted versus P_{VTIP} measured at 5 K and 300 K. Within the growth window, the resistivity at 5 K was found to vary less than 30%, whereas at the edge of the window towards V-rich growth condition ($P_{VTIP} = 52.0$–52.5 mTorr), ρ(5 K) was found to vary by over

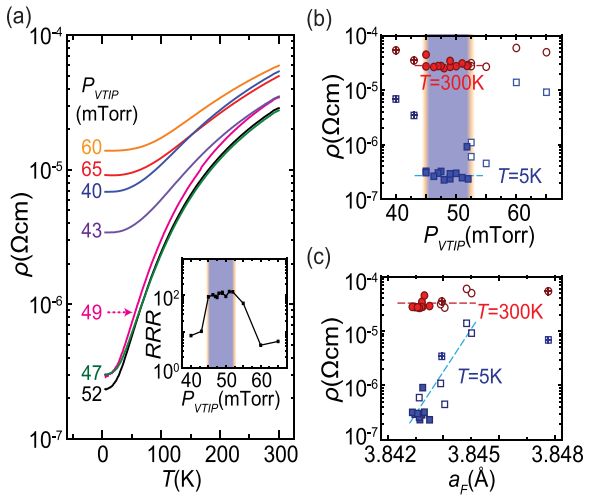

FIG. 3. (a) Resistivity versus temperature over the full range of P_{VTIP}. The inset shows the residual resistivity ratio $RRR = \rho(300\,\mathrm{K})/\rho(5\,\mathrm{K})$ versus P_{VTIP}. The shaded area indicates the growth window. (b) The resistivity at 300 K (red circles) and at 5 K (blue squares) plotted versus P_{VTIP}. Different filling indicate the different types of growth conditions: crossed—Sr-rich, filled—stoichiometric, and open—V-rich. (c) The resistivity at 300 K (red circles, symbols correspond to those in (b)) and at 5 K (blue squares) plotted versus the intrinsic lattice parameter. The trends are indicated by dashed lines as a guide to the eye.

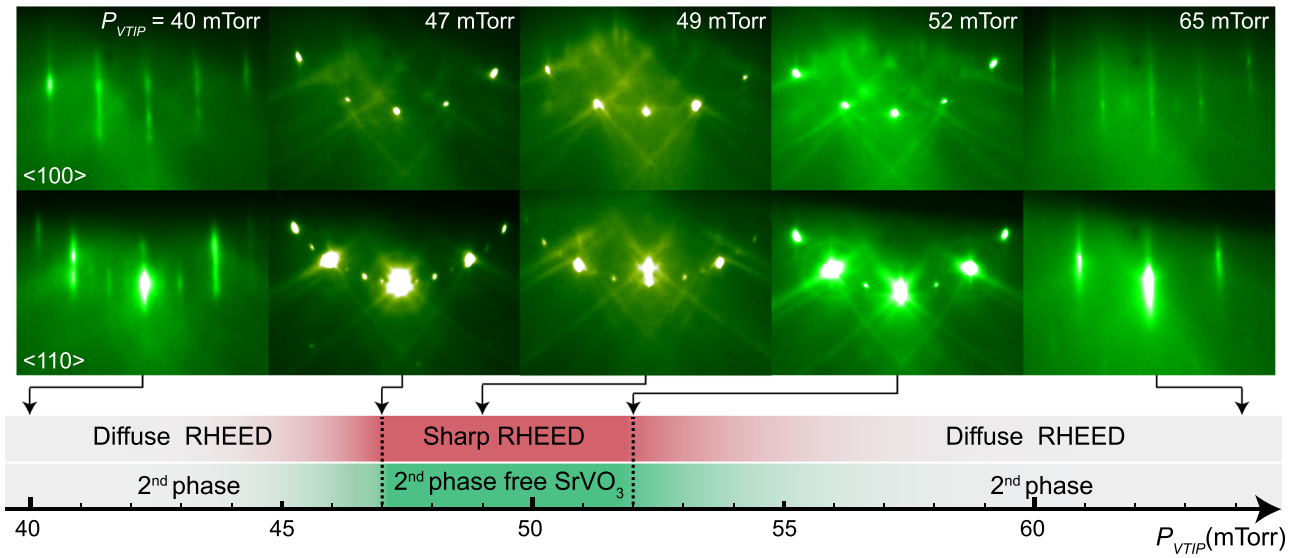

FIG. 4. Reflection high-energy electron diffraction images taken along the [100] (top row), and the [110] (bottom row) azimuth at 150 °C for films grown at various P_{VTIP}. The outer two (P_{VTIP} = 40.0 and 65.0 mTorr) were taken outside the growth window showing diffuse patterns and extra crystal phases,[32] and the inner three were taken inside the growth window $P_{VTIP} \approx 45.0$–52.0 mTorr, which showed sharp diffraction patterns with no sign of additional crystalline phases.

1000%. This large variation for the nominally same P_{VTIP} was attributed to the small uncertainties in the relative Sr flux (±2% according to film thickness variation), in excellent agreement with XRD. The high temperature resistivity was nearly independent of P_{VTIP}, and was only found to increase by a factor of ~2 for films grown under grossly non-stoichiometric conditions, while the low temperature resistivity was found to vary by nearly two orders of magnitude. The low temperature resistivity is dominated by defect scattering, while electron-phonon scattering is the main contribution to the room temperature resistivity and only increases when phonon and defect scattering have the same magnitude, which renders ρ(5 K) and *RRR* as very sensitive probes of stoichiometry for $SrVO_3$. The weak dependence on disorder at room temperature is beneficial by allowing less restrictive tolerances to harness the low room temperature resistivity of $SrVO_3$, ranging between 2.5 and 5.0×10^{-5} Ω·cm, for practical applications, such as bottom electrode for functional perovskite oxides.[6]

We have further linked the two measures of nonstoichiometry and defect density in the $SrVO_3$—intrinsic film lattice parameter and resistivity—by plotting ρ(300 K) and ρ(5 K) as a function of lattice parameter for P_{VTIP} varying over the full range from 40.0 to 65.0 mTorr in Fig. 3(c). For the resistivity measured at 5 K, a very high sensitivity to defect-induced expansion of the lattice was found. As highlighted by the dashed curve, the low temperature resistivity ρ(5 K) increased exponentially with increasing film lattice parameter, almost two orders in magnitude within a lattice parameter expansion as small as ~4 pm (~1%), which shows the low temperature resistivity is an extremely precise measure for defect concentration. All samples grown inside the growth window with $P_{VTIP} \approx 45.0$–52.0 mTorr (filled squares) were tightly clustered at low temperature resistivity values around 0.2–0.3 μΩ·cm and small lattice parameter $a_F = 3.843$ Å. This further confirms that inside the growth window the samples are stoichiometric and insensitive to P_{VTIP}.

Finally, *in situ* reflection high-energy electron diffraction (RHEED) measurements further supported the existence of a growth window.[35,36] Figure 4 shows RHEED images taken along the ⟨110⟩ and ⟨100⟩ directions after depositing ~50 nm of $SrVO_3$ at ~900 °C, and cooling down to ~150 °C. For $P_{VTIP} \approx 45.0$–52.0 mTorr, films were highly crystalline with smooth surfaces. Diffraction images consistently showed bright intensity reflections confined to the Laue circles rather than a streaky pattern, as well as sharp Kikuchi lines. For $P_{VTIP} > 52.0$ mTorr or <45.0 mTorr, RHEED patterns became more diffuse, the diffraction spots elongated along the vertical direction and the Kikuchi patterns disappeared. Furthermore, the films showed a 4-fold reconstruction along ⟨110⟩. While a 4-fold reconstruction along ⟨110⟩ was still observed for films grown under Sr-rich conditions, it transitioned to a 2-fold reconstruction and finally disappeared for films grown under V-rich conditions. Therefore, unlike $SrTiO_3$,[36] the surface reconstructions in $SrVO_3$ seem to not be as sensitive to the underlying stoichiometry of the films. However, for films with $P_{VTIP} > 52.0$ or <47.0 mTorr, RHEED images taken during sample rotation revealed additional reflections not characteristic of $SrVO_3$.[32] These extra reflections were attributed to the presence of parasitic phases on the film surface, likely rock salt SrO (Sr-rich) and VO_x (V-rich).[13] It is interesting to note that the window for $P_{VTIP} = 47.0$–52.0 mTorr where the film surfaces were free of such secondary phase features was narrower on the Sr-rich side than defined by the less surface-sensitive XRD and transport measurements ($P_{VTIP} = 45.0$–52.0 mTorr). This suggests that SrO defects formed already for $P_{VTIP} < 47.0$ mTorr (slightly Sr-rich) and were floating on the surface,[37,38] while only for P_{VTIP} below 45 mTorr (extremely Sr-rich) they were incorporated into the bulk of the film.

In conclusion, the favorable growth conditions attainable in hMBE can also be harnessed for the growth of $SrVO_3$. It was shown that stoichiometric films can be grown

over a wide range of Sr/VTIP fluxes leaving defect sensitive properties, the intrinsic lattice parameter and low temperature resistivity, unaffected. The discovery that a self-regulated growth window can be accessed for $SrVO_3$ impacts both the fundamental research of this strongly correlated material, as well as showing a pathway to wafer scale production of $SrVO_3$ as an electrode material using a $SrTiO_3$ template on Si.[39] The existence of a growth window for an oxide compound without volatile constituents when grown by hMBE further indicates the general applicability of this growth approach to enable the synthesis of complex oxide thin films with excellent stoichiometric control, simply by introducing a volatile metal-organic precursor into the growth process.

M.B. and R.E.H. acknowledge the Department of Energy (Grant No. DE-SC0012375) for the growth, XRD, transport measurements, and preparation of the manuscript. C.E., L.Z., and H.T.Z. assisted in the growth and acknowledge support by the Office of Naval Research (Grant No. N00014-11-1-0665, L.Z. and R.E.H.), the National Science Foundation through the Penn State MRSEC Program DMR-1420620 (H.T.Z. and R.E.H.) as well as NSF Career Grant No. DMR-1352502 (C.E. and R.E.H.).

[1]Y. Tokura, Phys. Today **56**(7), 50 (2003).
[2]P. A. Lee and X.-G. Wen, Rev. Mod. Phys. **78**, 17 (2006).
[3]M. Imada, A. Fujimori, and Y. Tokura, Rev. Mod. Phys. **70**, 1039 (1998).
[4]J. M. Tomczak and S. Biermann, Phys. Status Solidi **246**, 1996 (2009).
[5]E. Morosan, D. Natelson, A. H. Nevidomskyy, and Q. Si, Adv. Mater. **24**, 4896 (2012).
[6]J. A. Moyer, C. Eaton, and R. Engel-Herbert, Adv. Mater. **25**, 3578 (2013).
[7]A. Fujimori, I. Hase, H. Namatame, Y. Fujishima, Y. Tokura, K. Takegahara, and F. M. F. de Groot, Phys. Rev. Lett. **69**, 1796 (1992).
[8]W. C. Sheets, B. Mercey, and W. Prellier, Appl. Phys. Lett. **91**, 192102 (2007).
[9]D. L. Ritums, N. J. Wu, D. Liu, Q. Zhong, Y. M. Chen, X. Zhang, P. C. Chou, and A. Ignatiev, in *Proceedings of the Tenth IEEE International Symposium on Applications of Ferroelectrics (ISAF)* (IEEE, 1996), pp. 417–420.
[10]H. Nagata, T. Tsukahara, M. Yoshimoto, and H. Koinuma, Thin Solid Films **208**, 264 (1992).
[11]P. W. Yip and K. H. Wong, MRS Proc. **623**, 347 (2000).
[12]M. Gu, S. A. Wolf, and J. Lu, Adv. Mater. Interfaces **1**, 1300126 (2014).
[13]C. Eaton, J. A. Moyer, H. M. Alipour, E. D. Grimley, M. Brahlek, J. M. LeBeau, and R. Engel-Herbert, J. Vac. Sci. Technol., A **33**, 061504 (2015).
[14]K. Byczuk, W. Hofstetter, and D. Vollhardt, Phys. Rev. Lett. **94**, 056404 (2005).
[15]P. A. Lee, Rev. Mod. Phys. **57**, 287 (1985).
[16]W. P. McCray, Nat. Nanotechnol. **2**, 259 (2007).
[17]J. Y. Tsao, *Materials Fundamentals of Molecular Beam Epitaxy* (Academic Press, Inc., San Diego, 1993).
[18]L. Pfeiffer and K. W. West, Phys. E **20**, 57 (2003).
[19]J. F. Ihlefeld, A. Kumar, V. Gopalan, D. G. Schlom, Y. B. Chen, X. Q. Pan, T. Heeg, J. Schubert, X. Ke, P. Schiffer, J. Orenstein, L. W. Martin, Y. H. Chu, and R. Ramesh, Appl. Phys. Lett. **91**, 071922 (2007).
[20]C. D. Theis, J. Yeh, D. G. Schlom, M. E. Hawley, and G. W. Brown, Thin Solid Films **325**, 107 (1998).
[21]J. H. Lee, X. Ke, R. Misra, J. F. Ihlefeld, X. S. Xu, Z. G. Mei, T. Heeg, M. Roeckerath, J. Schubert, Z. K. Liu, J. L. Musfeldt, P. Schiffer, and D. G. Schlom, Appl. Phys. Lett. **96**, 262905 (2010).
[22]B. Jalan, P. Moetakef, and S. Stemmer, Appl. Phys. Lett. **95**, 032906 (2009).
[23]J. N. Eckstein and I. Bozovic, Annu. Rev. Mater. Sci. **25**, 679 (1995).
[24]B. Jalan, R. Engel-Herbert, J. Cagnon, and S. Stemmer, J. Vac. Sci. Technol., A **27**, 230 (2009).
[25]R. Engel-Herbert, *Molecular Beam Epitaxy* (Elsevier, 2013), pp. 417–449.
[26]H. Koinuma, M. Yoshimoto, H. Nagata, and T. Tsukahara, Solid State Commun. **80**, 9 (1991).
[27]W. T. Tsang, J. Cryst. Growth **95**, 121 (1989).
[28]H. Lüth, Surf. Sci. **299–300**, 867 (1994).
[29]J. Son, P. Moetakef, B. Jalan, O. Bierwagen, N. J. Wright, R. Engel-Herbert, and S. Stemmer, Nat. Mater. **9**, 482 (2010).
[30]P. Xu, D. Phelan, J. S. Jeong, K. A. Mkhoyan, and B. Jalan, Appl. Phys. Lett. **104**, 082109 (2014).
[31]H.-T. Zhang, L. R. Dedon, L. W. Martin, and R. Engel-Herbert, Appl. Phys. Lett. **106**, 233102 (2015).
[32]See supplementary material at http://dx.doi.org/10.1063/1.4932198 for experimental methods and extended RHEED analysis.
[33]J. M. LeBeau, R. Engel-Herbert, B. Jalan, J. Cagnon, P. Moetakef, S. Stemmer, and G. B. Stephenson, Appl. Phys. Lett. **95**, 142905 (2009).
[34]T. Ohnishi, K. Shibuya, T. Yamamoto, and M. Lippmaa, J. Appl. Phys. **103**, 103703 (2008).
[35]C. T. Foxon, Appl. Surf. Sci. **50**, 28 (1991).
[36]A. P. Kajdos and S. Stemmer, Appl. Phys. Lett. **105**, 191901 (2014).
[37]J. H. Lee, G. Luo, I. C. Tung, S. H. Chang, Z. Luo, M. Malshe, M. Gadre, A. Bhattacharya, S. M. Nakhmanson, J. A. Eastman, H. Hong, J. Jellinek, D. Morgan, D. D. Fong, and J. W. Freeland, Nat. Mater. **13**, 879 (2014).
[38]Y. F. Nie, Y. Zhu, C.-H. Lee, L. F. Kourkoutis, J. A. Mundy, J. Junquera, P. Ghosez, D. J. Baek, S. Sung, X. X. Xi, K. M. Shen, D. A. Muller, and D. G. Schlom, Nat. Commun. **5**, 4530 (2014).
[39]L. Zhang and R. Engel-Herbert, Phys. Status Solidi RRL **8**, 917 (2014).